scientific reports

Check for updates

OPEN

Minocycline alleviates lipopolysaccharide-induced cardiotoxicity by suppressing the NLRP3/Caspase-1 signaling pathway

Huijuan Li[1], Xiaozhong Li[2,4], Guohai Xu[3] & Fenfang Zhan[3,4]✉

Minocycline (Min), as an antibiotic, possesses various beneficial properties such as anti-inflammatory, antioxidant, and anti-apoptotic effects. Despite these known qualities, the precise cardioprotective effect and mechanism of Min in protecting against sepsis-induced cardiotoxicity (SIC) remain unspecified. To address this, our study sought to assess the protective effects of Min on the heart. Lipopolysaccharide (LPS) was utilized to establish a cardiotoxicity model both in vivo and in vitro. Min was pretreated in the models. In the in vivo setting, evaluation of heart tissue histopathological injury was performed using hematoxylin and eosin (H&E) staining and TUNEL. Immunohistochemistry (IHC) was employed to evaluate the expression levels of NLRP3 and Caspase-1 in the heart tissue of mice. During in vitro experiments, the viability of H9c2 cells was gauged utilizing the CCK8 assay kit. Intracellular ROS levels in H9c2 cells were quantified using a ROS assay kit. Both in vitro and in vivo settings were subjected to measurement of oxidative stress indexes, encompassing glutathione (GSH), malondialdehyde (MDA), and superoxide dismutase (SOD) levels. Additionglly, myocardial injury markers like lactate dehydrogenase (LDH) and creatine kinase MB (CK-MB) activity were quantified using appropriate assay kits. Western blotting (WB) analysis was conducted to detect the expression levels of NOD-like receptor protein-3 (NLRP3), caspase-1, IL-18, and IL-1β, alongside apoptosis-related proteins such as Bcl-2 and Bax, and antioxidant proteins including superoxide dismutase-1 (SOD-1) and antioxidant proteins including superoxide dismutase-1 (SOD-2), both in H9c2 cells and mouse heart tissues. In vivo, Min was effective in reducing LPS-induced inflammation in cardiac tissue, preventing cell damage and apoptosis in cardiomyocytes. The levels of LDH and CK-MB were significantly reduced with Min treatment. In vitro studies showed that Min improved the viability of H9C2 cells, reduced apoptosis, and decreased ROS levels in these cells. Further analysis indicated that Min decreased the protein levels of NLRP3, Caspase-1, IL-18, and IL-1β, while increasing the levels of SOD-1 and SOD-2 both in vivo and in vitro. Min alleviates LPS-induced SIC by suppressing the NLRP3/Caspase-1 signalling pathway in vivo and in vitro.

Keywords Sepsis, Cardiotoxicity, Lipopolysaccharide, NLRP3/Caspase-1 pathway, Minocycline

Sepsis, a condition characterized by systemic inflammation stemming from infection, can cause dysfunction multiple organs[1]. Among its common complications, sepsis-induced cardiomyopathy (SIC) stands out as a critical factor that significantly impacts the patient's health and prognosisis[2,3]. In adult sepsis patients, the incidence of myocardial injury ranges from 25 to 50%, serving as a significant indicator of poor prognosis and potentially leading to a mortality rate of 70%[4]. Given these alarming statistics, it is imperative to explore strategies to mitigate the effects of SIC.

[1]Department of Anesthesiology, Wuhan Third Hospital, Wuhan 430074, China. [2]Department of Cardiovascular Medicine, The Second Affiliated Hospital of Nanchang University, Nanchang, 330006, China. [3]Department of Anesthesiology, The Second Affiliated Hospital of Nanchang University, Nanchang 330006, China. [4]Jiangxi Key Laboratory of Molecular Medicine, Nanchang, 330006, China. ✉email: 499802609@qq.com

Various mechanisms, such as mitochondrial damage, oxidative stress, metabolic imbalance, and inflammation, have been identified as playing a role in the development of sepsis-induced cardiac dysfunction[5,6]. Among these mechanisms, inflammation and oxidative damage are highlighted as key factors in the pathogenesis of septic cardiomyopathy[7,8]. In sepsis, the excessive release of pro-inflammatory cytokines like tumor necrosis factor-alpha (TNF-α) and interleukins (ILs) into the bloodstream triggers an immune response in the heart muscle, leading to the production of reactive oxygen species (ROS) and ultimately causing myocardial cell apoptosis[9]. Therefore, it is crucial to target the inhibition of inflammatory response and ROS generation in order to effectively treat septic cardiomyopathy.

The NOD-like receptor family pyrin domain-containing 3 (NLRP3) inflammasome, consisting of NLRP3, apoptosis-associated speck-like protein (ASC), and caspase-1, boots the production of proinflammatory cytokines[10]. Upon activation, NLRP3 creates a complex that triggers caspase-1, leading to the conversion of procytokines, like ASC, Interleukin-1 beta (IL-1β) into mature forms, thereby promoting inflammation[11,12]. Recent scientific investigations underscore the pivotal role of NLRP3 activation in initiating and perpetuating the inflammatory cascade in septic cardiomyopathy[13]. Therefore, targeting NLRP3 shows promise as a strategy against SIC.

Minocycline (Min), a member of the tetracycline antibiotic class, is renowned for its multifaceted properties, encompassing anti-inflammatory, anti-apoptotic, and immunomodulatory actions[14–16]. Mahmoud et al. demonstrated that Min effectively reduced sepsis-induced memory impairment in mice with sepsis-associated encephalopathy[17]. Furthermore, another study has unveiled Min's potential to alleviate doxorubicin(DOX)-induced cardiotoxicity by combating inflammation and oxidative stress[18]. Nevertheless, the specific impact of Min on sepsis-triggered myocardial dysfunction remains an unexplored territory. The current investigation delves into the influence of Min and its mechanism in LPS-induced SIC in mice and LPS-induced H9c2 cells.

Materials and methods

Drugs and regent

LPS (#L2880, *Escherichia coli* 055: B5) and Minocycline hydrochloride (#M9511) were acquired from Sigma Aldrich Company (Sigma Aldrich Co., USA). According to the product specifications and privious studies[19,20], the LPS powder was dissolved with sterile normal saline. The LPS concentration for animal experiments was formulated as: 5 mg/ml. The LPS concentration for cell experiments was formulated as 1 mg/ml. The prepared LPS was stored in a brown EP tube at -20℃. NLRP3(#ab270499), Caspase-1(#ab179515), IL-1β (#ab234437), IL-18(#ab243091), SOD-1(#ab51254), SOD-2(#ab68155) was purchased from Abcam (Cambridge, MA, USA). Bax (#50599-2-lg), Bcl-2 (68103-1-lg) and GAPDH (#60004-1-lg) were purchased from Proteintech (Wuhan, China).

Animals and treatment

The animal experiments were carried out following the Guidelines for the Care and Use of Laboratory Animals issued by the U.S. National Institute of Health. The study protocols were approved by the Institutional Animal Care and Use Committee at the Medical College of Nanchang University Approval for all in vivo experiments in this research was granted by the Animal Care and Use Committee at the Second Affiliated Hospital of Nanchang University (approval number: A20230425109). The principles established in the institutional guidelines were faithfully followed during the duration of this study.

Six- to seven-week-old C57BL/6J mice and weighting 25–30 g, sourced from Skobis company in Henan, China, were accommodated in the Nanchang University Animal Facility. The facility maintained an air-conditioned environment with a regulated 12-h light/dark cycle, with lights illuminated from 8:00 am to 8:00 pm. Each mouse was housed individually in polystyrene cages, ensuring unfettered access to both water and food at all times.

To study the effect of LPS-induced cardiotoxicity, animals were assigned to four groups (n = 6 per group): a control group, an LPS (10 mg/kg) group, an LPS (10 mg/kg) + Min(45 mg/kg) group, and an LPS (10 mg/kg) + Min(90 mg/kg) group. The control and LPS groups received intraperitoneal injections of normal saline, matching the volume and frequency of the Min injections in the respective treatment groups. The mice in the Min groups were injected intraperitoneally with Min for three consecutive days. On the third day, 1 h following the Min injection, the LPS groups (2, 3, 4) were challenged with 10 mg/kg LPS via intraperitoneal injection, while the control group received an equivalent volume of normal saline. The dosage of Min(45 mg/kg or 90 mg/kg) and LPS (10 mg/kg) falls within the range that has been previously reported in previous literature[21–24]. After intraperitoneally injecting mice with LPS, we recorded the number of mice alive in each group within 24 h. After 24 h of LPS treatment, the heart weight index (HWI) of mice was teated, according to privious report[25]. All animals were enthanized by intraperitoneally injecting 0.2 ml of 6% pentobarbital sodium, and then weighted. Subsequently, the heart tissues of mice were meticulously harvested, with meticulous exclusion of connective tissues and major blood vessels. These tissues were then blotted dry using filter paper, prior to their heart weight (HW) being accurately determined utilizing an electronic analytical balance. The HWI was computed as HW/BW. Then Blood and heart tissues samples were promptly collected and stored at −80 °C for subsequent analyses.

Heart tissue histopathology and immunohistochemical analysis

To validate cardiomyocyte morphology and the presence of inflammatory cell infiltration, Hematoxylin and Eosin (H&E) staining was executed on cardiac tissue samples that underwent paraformaldehyde fixation and paraffin embedding.

Following standard protocols, both TUNEL (Terminal deoxynucleotidyl transferase dUTP Nick End Labeling) and immunohistochemical (IHC) staining procedures were carried out. TUNEL staining specifically aimed to quantify TUNEL-positive cells, indicative of apoptotic activity, while IHC staining targeted the detection of

NLRP3 and Caspase-1 expressions. Positive TUNEL cells displayed green-hued nuclear granules, whereas NLRP3 and Caspase-1 protein expressions manifested as brown-yellow cytoplasmic granules.

For the acquisition and subsequent analysis of these stained images, a microscope coupled with ImageJ software was utilized.

Assay for LDH and CK-MB activity

The activity of lactate dehydrogenase (LDH) and myocardial-bound creatine kinase (CK-MB) in serum and cell supernatant was measured using an automated biochemical analyser (ADVIA2400; Sicemens) as previously described[26]. Enzyme activity was reported as U/L[27].

Cell culture and drug treatment

H9c2 cells, sourced from the Cell Bank of the Chinese Academy of Sciences in Shanghai, China, were cultured and maintained in Dulbecco's Modified Eagle's Medium (DMEM; Gibco, Logan, UT, USA), enriched with 10% fetal bovine serum (#04-001-1ACS, BI Co. Ltd, Israel). These cells were incubated at 37 °C, under conditions of 5% CO_2 and 95% O_2. Following established protocols[22,28], Min was introduced into the culture medium 2 h prior to administering LPS (1 μg/ml) for a duration of 24 h. Subsequently, the treated cells were harvested for further examination and analysis.

Cell viability assay

H9c2 cells were initially placed into 96-well Corning plates at a density of 5,000 cells per well using 100 μL of medium containing 10% FBS and incubated at 37 °C with 5% CO_2 for 24 h. Subsequently, the H9c2 cells were exposed to varying concentrations of Min (0, 10, 20, 40, 80, 160 μM) and/or LPS for another 24h period. Following this, the Cell Counting Kit-8 (CCK-8, #A311-02-A, Nanjing, China) solution was introduced to the 96-well plates with the H9c2 cells for a duration of 1 h. The absorbance at 450 nm was then measured utilizing a Beckman microplate reader in Shanghai, China.

Assay for intracellular ROS

Based on the CCK-8 assay outcomes, H9c2 cells were categorized into five distinct groups: (1) Control, (2) LPS-treated, (3) LPS + Min (10 μM), (4) LPS + Min (20 μM), and (5) LPS + Min (40 μM). To quantify intracellular ROS levels, the ROS assay kit (#S0033S, Beyotime, Shanghai) was employed. Adhering to the manufacturer's guidelines, 2′,7′-dichlorofluorescein diacetate (DCFH-DA) was diluted in serum-free medium at a 1:1000 ratio, resulting in a final concentration of 10 μM. An adequate volume of this DCFH-DA solution was then added to the H9c2 cells and incubated at 37 °C for 20 min. Following incubation, all groups were analyzed under a fluorescence microscope. ImageJ software (National Institutes of Health, Bethesda, MD) was utilized to assess and quantify the fluorescence intensity of ROS, thereby enabling the comparison of ROS levels across the different groups.

Analysis of oxidative stress

After cells were grouped as described above, the glutathione (GSH) level was evaluated using a GSH assay kit (#S0053), while the malondialdehyde (MDA) level and the superoxide dismutase (SOD) activity were detected using the Lipid Peroxidation MDA assay kit (#S0131S) and the SOD assay kit (#S0101S), respectively. The testing methods were strictly in accordance with the manufacturer's instructions. All the kits were purchased from Beyotime (Shanghai, China).

Immunofluorescence

The experiment started with the seeding of H9c2 cells in 6-well plates in a manner consistent with the outlined grouping technique. Subsequently, the cells underwent fixation using 4% paraformaldehyde, followed by permeabilization utilizing 0.1% Triton-X-100 and incubation in a 5% bovine serum albumin solution. Following this, the cells were subjected to staining with primary antibodies targeting NLRP3 and Caspase-1 overnight at 4 °C, and then were exposed to secondary antibodies at room temperature for 1 h. In the subsequent step, H9c2 cells were stained with DAPI for a duration of 10 min using product #AR1177 (Boster, China). A sealing tablet for anti-fluorescence quenching, identified by product #AR0036 (Boster, China), was employed to seal the resulting cell slide, while imaging of the cells was performed using a fluorescence microscope, specifically the Nikon NI-V.

Western blotting analysis

Protein lysates were extracted from both cultured H9c2 cells and cardiac tissue samples. Total protein concentrations in these samples were quantified using the BCA Kit (Tiangen, Beijing, China). The protein samples were then subjected to electrophoresis on 10% SDS-PAGE gels and transferred onto PVDF membranes. Overnight incubation at 4 °C with primary antibodies specific to NLRP3, Caspase-1, IL-1β, IL-18, SOD-1, SOD-2, Bax, Bcl-2 and GAPDH (at dilutions of 1:1000 and 1:2000 for GAPDH) was performed. Following TBST washes, the membranes were incubated with secondary antibodies for 1 h at room temperature. Chemiluminescence was induced using an ECL substrate solution (Proteintech, Wuhan, China) applied uniformly onto the membranes. Finally, the gray values of the bands were analyzed using ImageLab software for quantitative assessment.

Statistical analysis

All data values were represented as mean ± standard error of the mean (SEM). Results were analyzed by one-way ANOVA with Tukey's multiple comparison test using GraphPad Prism version 8.0. $P < 0.05$ was considered significant.

Results

Minocycline alleviated LPS-induced myocardial injury in mice.

As shown in Supplemental Fig. 1, Min preconditioning reduced the LPS-induced mortality and improved the survival rate of mice. Next, we assessed the effects of Min on LPS-induced heart damage. The results of H&E staining in the heart tissues of mice are shown in Fig. 1A. Relative to the control group, the hearts in the LPS-treated group displayed various histological changes, including a substantial infiltration of inflammatory cells, disrupted myocardium, and leakage of protein mucus. The hearts in the LPS + Min-treated group at 45 mg/kg exhibited reduced vacuolization and minimal inflammatory cell infiltration. Similarly, the hearts in the LPS + Min-treated group at 90 mg/kg showed minor inflammatory cell infiltration and maintained a normal organizational structure with negligible damage. Subsequently, we measured the levels of the cardiac injury markers CK-MB and LDH (Fig. 1B, C). Markedly elevated levels of CK-MB and LDH were observed in the LPS-treated group in comparison to the control group. Treatment with LPS + Min at 100 mg/kg resulted in a noticeable decrease in CK-MB and LDH levels compared to the LPS-treated group. Apoptosis in the heart tissue was assessed through Western blot and TUNEL staining. The Western blot outcomes (Fig. 1D–F) displayed a marked decrease in the expression of the anti-apoptosis protein Bcl-2 compared to the control group. Conversely, the LPS + Min-treated group at 100 mg/kg displayed enhanced Bcl-2 expression compared to the LPS-treated group, while the expression of the pro-apoptotic protein Bax exhibited an opposite trend to Bcl-2. The TUNEL staining results (Fig. 1G, H) indicated a higher level of cardiac apoptosis in the LPS-treated group compared to the control group. The introduction of LPS + Min at both 45 and 90 mg/kg significantly diminished the extent of cardiac apoptosis compared to the LPS-treated group. Besides, we evaluated the HWI in different groups of mice (Table 1). The results suggested that HWI were greater in the LPS-induced mice than that in the control group mice. With the pre-treatment of Min, HWI significantly decreased compared with that of LPS-induced mice. These findings underscore the potential of Min in mitigating LPS-induced myocardial injury in mice.

Minocycline inhibits LPS-induced oxidative stress in the mice heart

To evaluate the impact of Min on LPS-induced oxidative stress in the hearts of mice, we investigated the levels of oxidative stress markers and the expression of antioxidant proteins in various experimental group. As depicted in Fig. 2A–C, we observed the concentration of MDA significantly increased, whereas GSH and SOD activity levels significantly decreased in the LPS group relative to the control group. In contrast, the LPS + Min groups showed a pronounced reduction in MDA concentration and a notable increase in the GSH and SOD activity levels (both at 45 and 90 mg/kg) compared to the LPS group. Utilizing Western blotting, we assessed the levels of antioxidant proteins such as SOD-1 and SOD-2. The data depicted in Fig. 2D–F indicated a marked decrease in the expression of SOD-1 and SOD-2 in the LPS group compared to the control group. However, in the LPS + Min groups (at 90 mg/kg), there was a significant rise in the expression of SOD-1 and SOD-2 compared to the LPS group. These findings indicate that Min has the capability to suppress LPS-induced oxidative stress in the hearts of mice.

Minocycline inhibits LPS-induced NLRP3/Caspase-1 pathway activation in mice heart

The influence of Min on the NLRP3/Caspase-1 signaling cascade was evaluated through Western blot and IHC staining techniques. The results from Western blot analysis revealed a considerable elevation in the abundance of NLRP3, Caspase-1, IL-1β, and IL-18 proteins in the LPS group compared to the control group. Notably, pretreatment with Min significantly mitigated the expression of these proteins in the LPS + Min group, at both 45 and 90 mg/kg doses, as evident from Fig. 3A–E. Furthmore, IHC staining illuminated an upregulation of NLRP3 and Caspase-1 expression triggered by LPS in the LPS group, which was effectively counteracted by Min intervention in the LPS + Min group across both dosage, as depicted in Fig. 3F. Collectively, these observations underscore the efficacy of Min in suppressing LPS-induced activation of the NLRP3/Caspase-1 pathway in the heart of mice.

Minocycline attenuated LPS-induced H9c2 cell injury

The investigation into Min's effect on LPS-mediated cellular damage was conducted by assessing cell viability, LDH release, and cell apoptosis evaluations in vitro. Initially, H9c2 cells were exposed to a range of Min concentrations (0–160 μM) for 24 h, demonstrating a concentration-dependent suppression of cell survival and elevation of LDH at higher doses (80–160 μM). Contrastingly, low concentrations (0–40 μM) of Min showed no significant impact on the measured parameters (Fig. 4A–C). Subsequently, low concentrations of Min (0–40 μM) were employed in subsequent experiments. To establish a stable myocardial injury model in vitro, H9c2 cells were treated with 1 μg/ml LPS for 24 h according to our preliminary results (Supplementary Fig. 2) and previous studies[28–30]. Pre-treating H9c2 cells with Min for 2 h efficiently mitigated LPS-induced cellular harm and mortality in a dose-responsive manner, as evidence by changes in cell viability and LDH levels (Fig. 4D, E). These results highlight Min's potential in attenuating LPS-induced H9c2 cell injury.

Minocycline inhibited LPS-induced oxidative stress in vitro

The intracellular ROS concentrations in H9c2 cells were quantified utilizing a dedicated assay kit. Notably, the LPS-exposed group exhibited significantly elevated fluorescence intensity compared to the control group, yet the inclusion of Min in the LPS + Min group effectively mitigated this rise (Fig. 5A), suggesting a potent inhibitory action against LPS-stimulated ROS generation.

To further elucidate Min's influence on LPS-induced oxidative stress in H9c2 cells, key oxidative stress markers such as MDA, SOD, and GSH were assessed (Fig. 5B–D). LPS treatment alone led to a marked increase in MDA levels and a corresponding decrease in SOD activity and GSH content, indicative of oxidative stress. Conversely, Min treatment mitigated these effects, normalizing MDA levels and enhancing both SOD activity and GSH content.

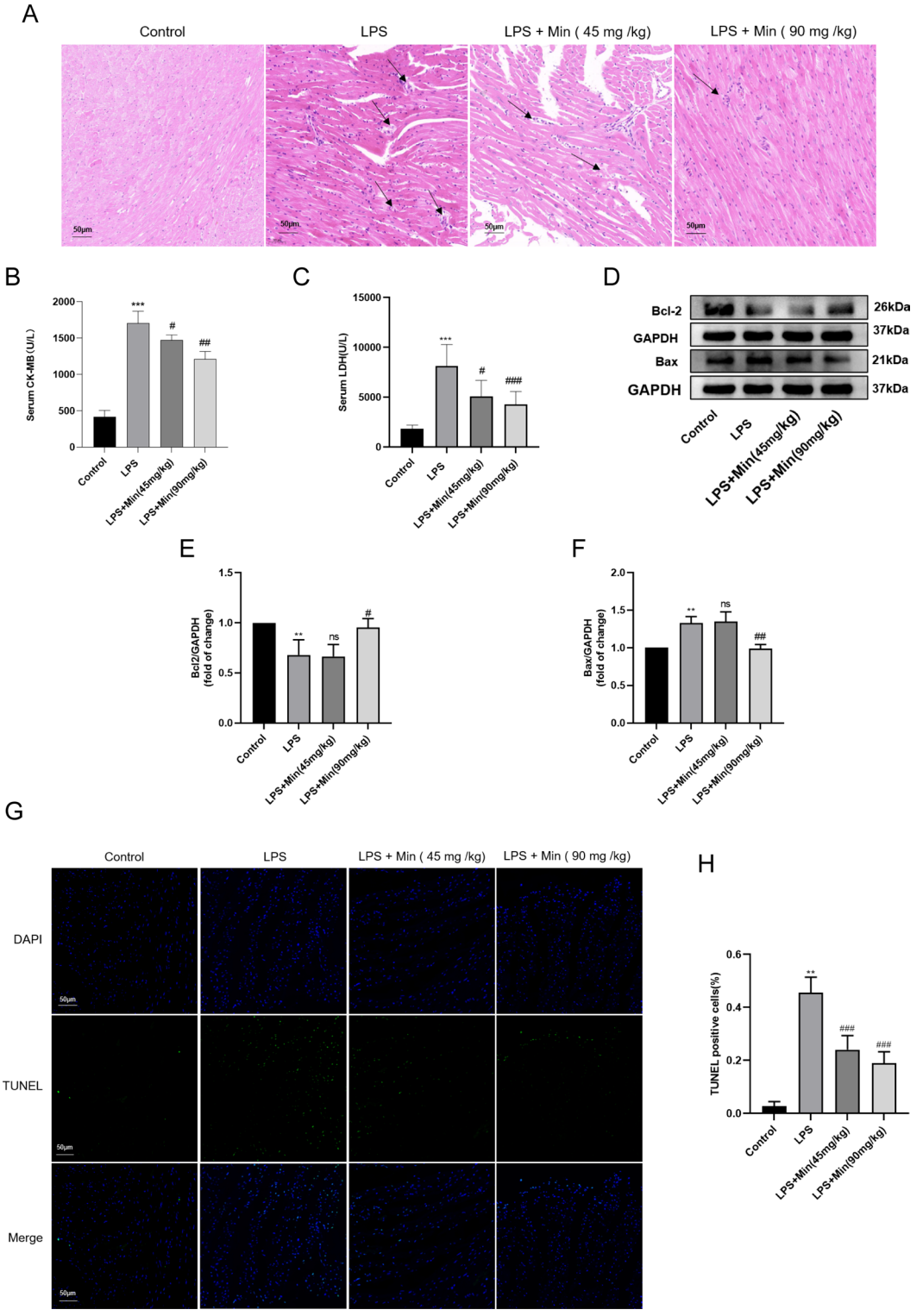

Fig. 1. Minocycline alleviated LPS-induced myocardial injury in mice. (**A**) Heart tissues were stained with H&E solution to elucidate pathological alterations. (**B,C**) The serum concentration of creatine kinase-MB (CK-MB) and lactate dehydrogenase (LDH) were detected. (**D–F**) The expression levels of Bax and Bcl-2 in mice heart tissues were detected by Weatern blotting assay. (**G,H**) TUNEL staining test was carried out to assess the apoptotics status in heart tissues. Data were presented as mean ± SD, n = 5–6 mice per group; ns: statistically non-significant; $^{*}P < 0.05$, $^{**}P < 0.01$, $^{***}P < 0.001$ vs. Control group; $^{\#}P < 0.05$, $^{\#\#}P < 0.01$, $^{\#\#\#}P < 0.001$ vs. LPS group.

Group	Number (n)	Heart weight (mg)	Body weight (g)	HWI (mg/g)
Control	6	114.37 ± 1.10	28.69 ± 1.34	3.99 ± 0.22
LPS	6	115.17 ± 1.17**	24.57 ± 1.14	4.68 ± 0.22**
LPS + Min(45 mg/kg)	6	114.57 ± 1.32#	27.17 ± 1.05	4.22 ± 0.17#
LPS + Min(90 mg/kg)	6	113.83 ± 1.68#	27.01 ± 1.12	4.24 ± 0.15#

Table 1. General characteristics of mice among different groups ($\bar{x} \pm SD$). $^{*}P < 0.05$, $^{**}P < 0.01$, $^{***}P < 0.001$ vs. Control group; $^{\#}P < 0.05$, $^{\#\#}P < 0.01$, $^{\#\#\#}P < 0.001$ vs. LPS group.

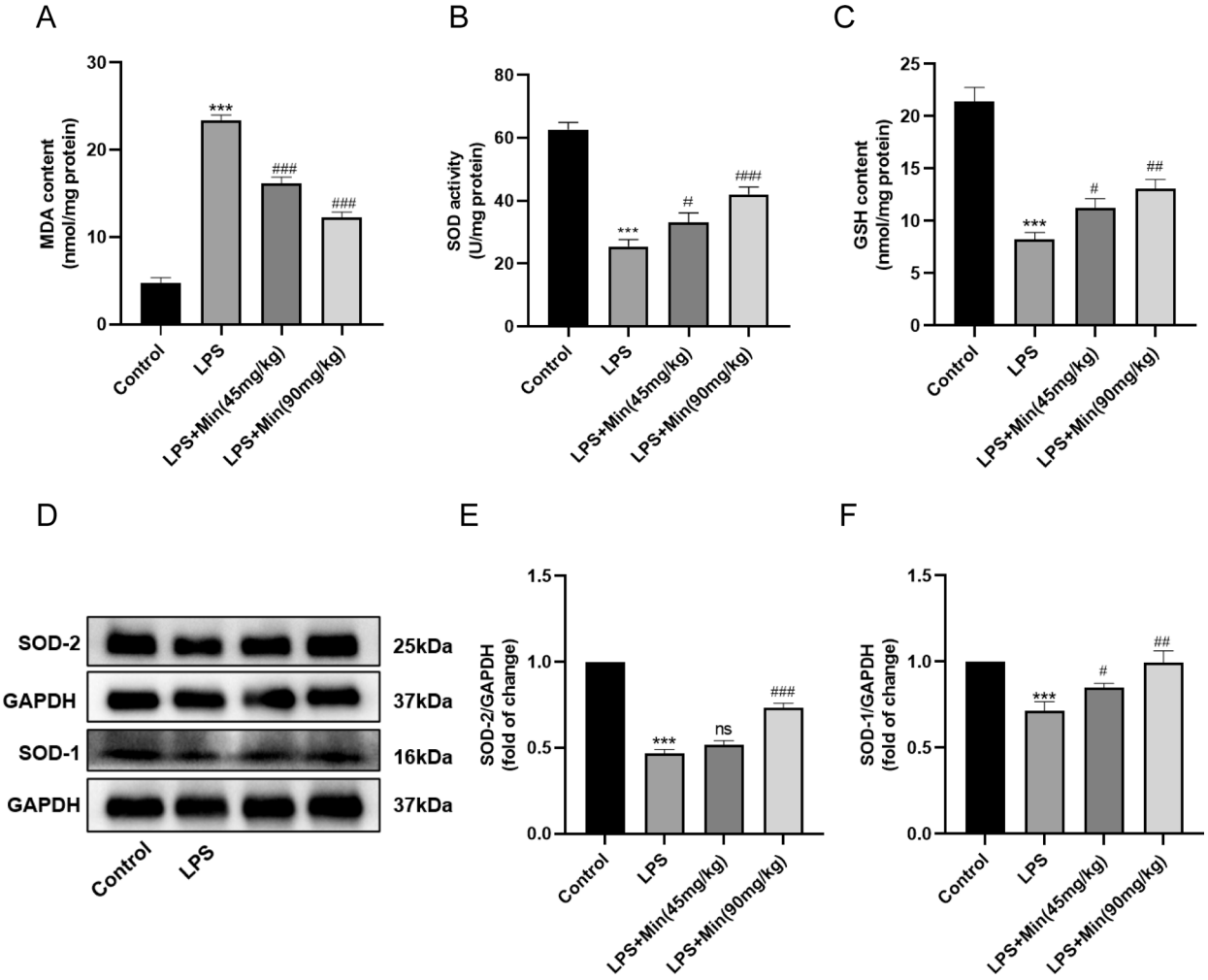

Fig. 2. Minocycline inhibits LPS-induced oxidative stress in the mice heart. (**A–C**) The levels of MDA, SOD, and GSH in mice heart tissues were detected by kit. (**D–F**) The antioxidant proteins SOD-1 and SOD-2 levels were identified by Western blotting assay. Data were presented as mean ± SD, n = 5–6 mice per group; ns: statistically non-significant; $^{*}P < 0.05$, $^{**}P < 0.01$, $^{***}P < 0.001$ vs. Control group; $^{\#}P < 0.05$, $^{\#\#}P < 0.01$, $^{\#\#\#}P < 0.001$ vs. LPS group.

Subsequent analysis focused on antioxidant protein expression, specifically SOD-1 and SOD-2 (Fig. 5E–G). Compared to the control, the LPS group displayed a significant downregulation of these proteins. However, pretreatment with Min induced a dose-dependent upregulation of SOD-1 and SOD-2 in the LPS + Min group. These observations underscore Min's potential as an effective modulator of LPS-mediated oxidative stress in vitro.

Minocycline inhibits LPS-induced NLRP3/Caspase-1 signaling pathway activation in H9c2 cells

Our study focused on investigating the effects of Min on the NLRP3/Caspase 1 signaling cascade in LPS-stimulated H9c2 cells. Using Western blotting and immunofluorescence staining, we analyzed the levels of NLRP3, Caspase-1, IL-1β, and IL-18 in different experimental groups. Notably, Fig. 6A–E demonstrates elevated protein levels of NLRP3, Caspase-1, IL-1β, and IL-18 in the LPS-treated group compared to the untreated control, with a subsequent reduction upon pre-treatment with minocycline in the LPS + Min group. Additionally,

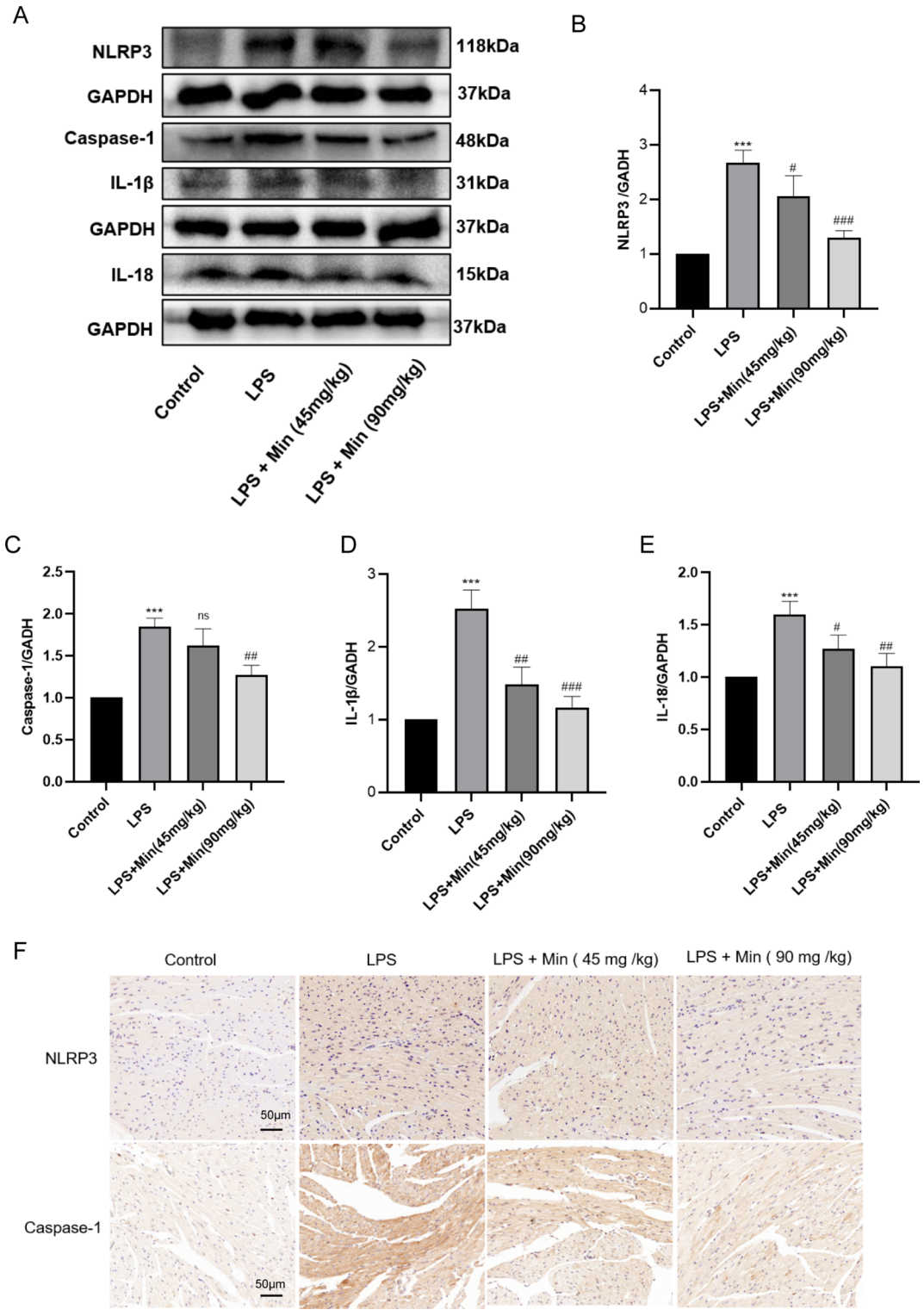

Fig. 3. Minocycline inhibits LPS-induced NLRP3/Caspase-1 pathway activation in mice heart. (**A**) Representative Western blot bands of NLRP3, Caspase-1, IL-1β, and IL-18, and (**B–E**) their statistical graphs. (**F**) An IHC staining assay was performed to detect the levels of NLRP3 and Caspase-1 in heart tissues. Data were presented as mean ± SD, n = 5–6 mice per group; ns: statistically non-significant; $^{*}P<0.05$, $^{**}P<0.01$, $^{***}P<0.001$ vs. Control group; $^{\#}P<0.05$, $^{\#\#}P<0.01$, $^{\#\#\#}P<0.001$ vs. LPS group.

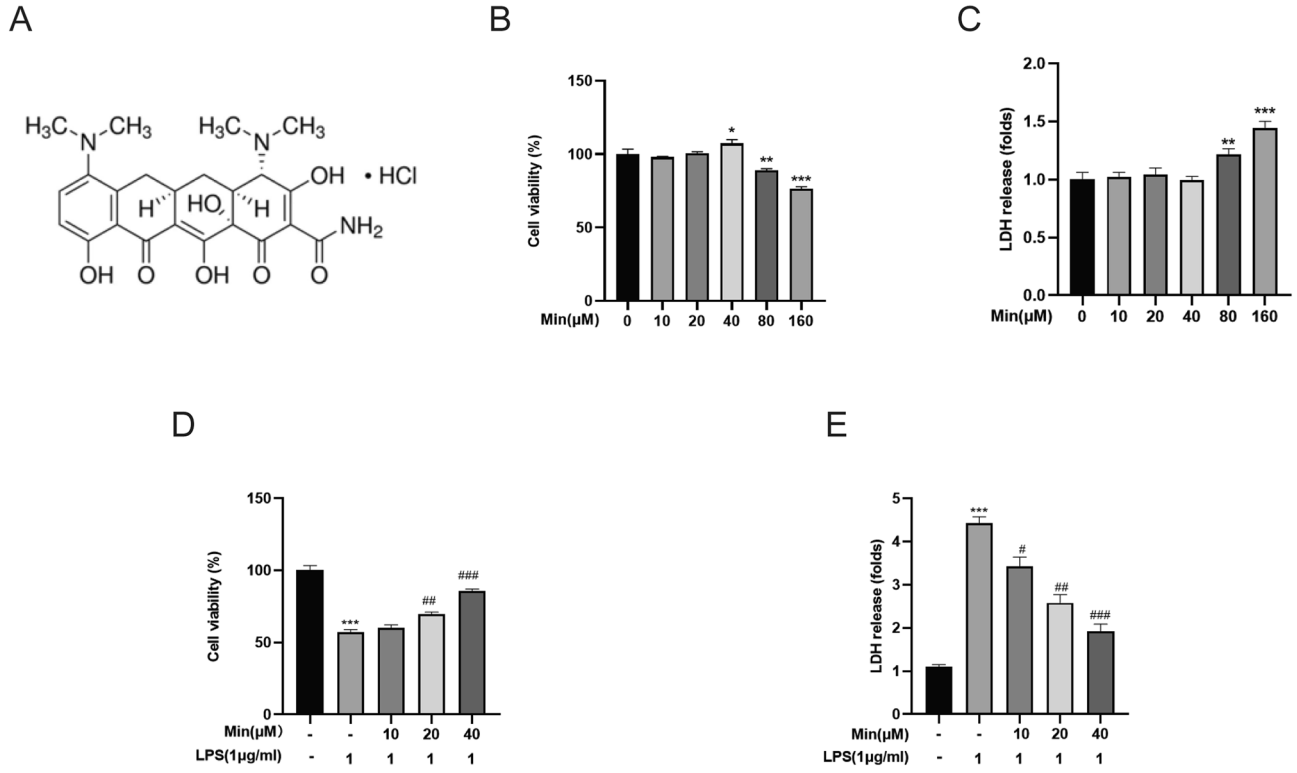

Fig. 4. Minocycline attenuated LPS-induced H9c2 cell injury. (**A**) Chemical structure of minocycline. (**B**) Cells were treated with 0–160 μM Min for 24 h, and cell viability was detected by the CCK-8 assay. (**C**) LDH level was measured in Min-treated H9c2 cells. (**D**) Min improved cell viability in LPS-treated H9c2 cells. (**E**) Min decreased LDH release in LPS-treated H9c2 cells. Data were presented as mean ± SD; n = 3; $^{*}P < 0.05$, $^{**}P < 0.01$, $^{***}P < 0.001$ vs. control group; $^{\#}P < 0.05$, $^{\#\#}P < 0.01$, $^{\#\#\#}P < 0.001$ vs. LPS group.

immunofluorescence staining illuminated an enhanced expression of both NLRP3 and Caspase-1 subsequent to LPS exposure, which was mitigated in a dose-responsive manner upon co-treatment with Min and LPS, as evident in Fig. 6F. Quantitative analysis further confirmed Min's inhibitory effect on NLRP3 and Caspase-1 expression (Fig. 6G, H), aligning with the Western blotting data. Collectively, these cumulative results support the conclusion that Min effectively inhibits the activation of the LPS-induced NLRP3/Caspase-1 signaling pathway in H9c2 cells.

Discussion

In this pioneering study, we illustrated for the first time the protective efficacy of Min in SIC. Our findings reveal that Min markedly mitigates cardiac injury in sepetic mice models, effectively ameliorating both in vivo and in vitro cardiomyocyte inflammation, oxidative stress, and apoptosis induced by LPS. Furthermore, Min potently inhibits LPS-mediated upregulation of NLRP3/Caspase-1 pathway components and proinflammatory cytokines, namely IL-1β and IL-18. In essence, our research underscores the potential of Min in alleviating LPS-induced cardiac dysfunction via suppression of the NLRP3/Caspase-1 signaling cascade.

SIC, a multifaceted disease, manifests itself through the malfunctioning of heart tissue. Its development is attributed to a range of factors, encompassing bacteria and diverse toxins[31] and sepsis serves as a crucial factor in the development of SIC[32]. LPS, a critical constituent of cell walls, capable of inducing severe sepsis and multi-organ dysfunctions when released into the blood stream[33,34]. Consequently, LPS is extensively utilized in laboratory settings to model sepsis, facilitating the exploration of its specific impacts on vital organs like the heart, brain, kidneys, and liver[35–38]. Based on previous studies of LPS in mice and H9c2 cells[23,28], this study meticulously conducted both in vivo and in vitro experiments. Our findings align with previous studies[39,40], demonstrating that following LPS administration, key cardiac injury biomarkers, CK-MB and LDH, exhibited elevated levels. In addition, we observed decreased cell viability and increased LDH release H9c2 cells with LPS, confirming the successful establishment of SIC models both in vivo and in vitro.

Recent investigations have underscored the pivotal role of Min in modulating inflammation and oxidative stress. Prior research has indicated that Min exerts its neuroprotective effects by suppressing neuroinflammation through deactivation of microglia, hindering the recruitment of inflammatory cells, and inhibiting the secretion of inflammation cytokines, thereby mitigating cognitive dysfunction[41]. Min also shows anti-oxidant and anti-inflammatory properties to reduce Dox-induced cardiotoxicity[18]. Besides, reportedly, Min can attenuate septic lung injury by inhibiting oxidative and inflammatory[42]. In our current study, we observed that Min treatment significantly inhibited inflammatory cell infiltration and apoptosis of cardiac muscle cells, accompanied by a decrease in the expression levels of CK-MB, LDH and MDA, alongside an upregulation of anti-oxidant proteins SOD-1 and SOD-2 and GSH, both in vitro and in vivo. In addition, Min also improved SOD activity in both

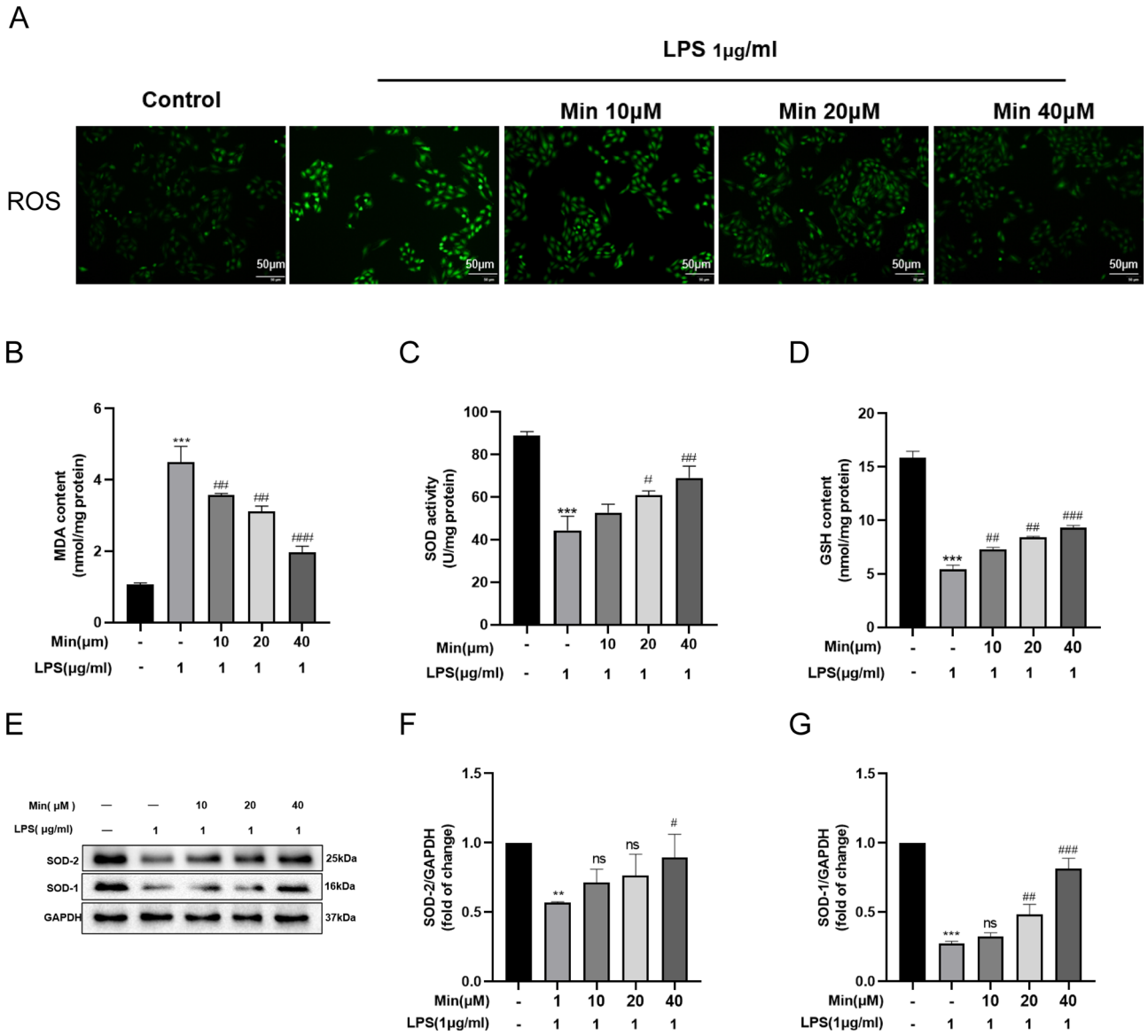

Fig. 5. Minocycline inhibited LPS-induced oxidative stress in vitro. (**A**) ROS kit was used to evaluated oxidative stress levels in H9c2 cells. (**B–D**) The levels of MDA, SOD, and GSH in H9c2 cells were detected by kit. (**E**) Representative Western blot bands of SOD-1 and SOD-2 and (**F,G**) their statistical graphs. Data were presented as mean ± SD; n = 3; ns: statistically non-significant; $^{*}P < 0.05$, $^{**}P < 0.01$, $^{***}P < 0.001$ vs. control group; $^{\#}P < 0.05$, $^{\#\#}P < 0.01$, $^{\#\#\#}P < 0.001$ vs. LPS group.

experimental settings. These comprehensive findings suggest that Min holds great promise as a therapeutic agent for sepsis-induced SIC.

Systemic inflammation resulting from sepsis triggers the activation of endogenous pathogen-associated molecular patterns (PAMPs) and damage-associated molecular patterns (DAMPs). By recognizing specific pathogen features via pattern recognition receptors (PRRs), the body initiates the release of a variety of inflammatory mediators, setting off an inflammatory cascade[43]. Studies have found that potential triggers of this SIC to include PAMPs like LPS, lipid cholic acid. These mediators interact with PRRs, activating intracellular signal transduction pathways, which then initiate an inflammatory cascade producing multiple inflammatory cytokines including TNF-α, IL-6, IL-18, and IL-1β[44,45]. The activation of the NLRP3 inflammasome promotes the activation of Caspase-1, as well as the maturation and secretion of IL-18 and IL-1β, leading to inflammation and cell necrosis[46]. Increasing evidence indicates that that activation of the NLRP3 inflammasome significantly affects myocardial function in septic heart disease. According to Zhang et al.[47] inhibiting the NLRP3 activation in cardiac fibroblasts mitigates LPS-induced myocardial dysfunction in mice, enhancing sepsis survival rates. Similarly, Yang et al.[48] found that down-regulating NLRP3 expression in setic rats reduces the release of downstream inflammatory factors, thereby ameliorating cardiac dysfunction. Thus, NLRP3 inhibition plays a critical role in treating septic heart disease. In our study, findings revealed that Min pretreatment markedly reduced the expression of NLRP3/Caspase-1 and inflammatory cytokines both in vivo and in vitro. Additionally, Min pretreatment was observed to

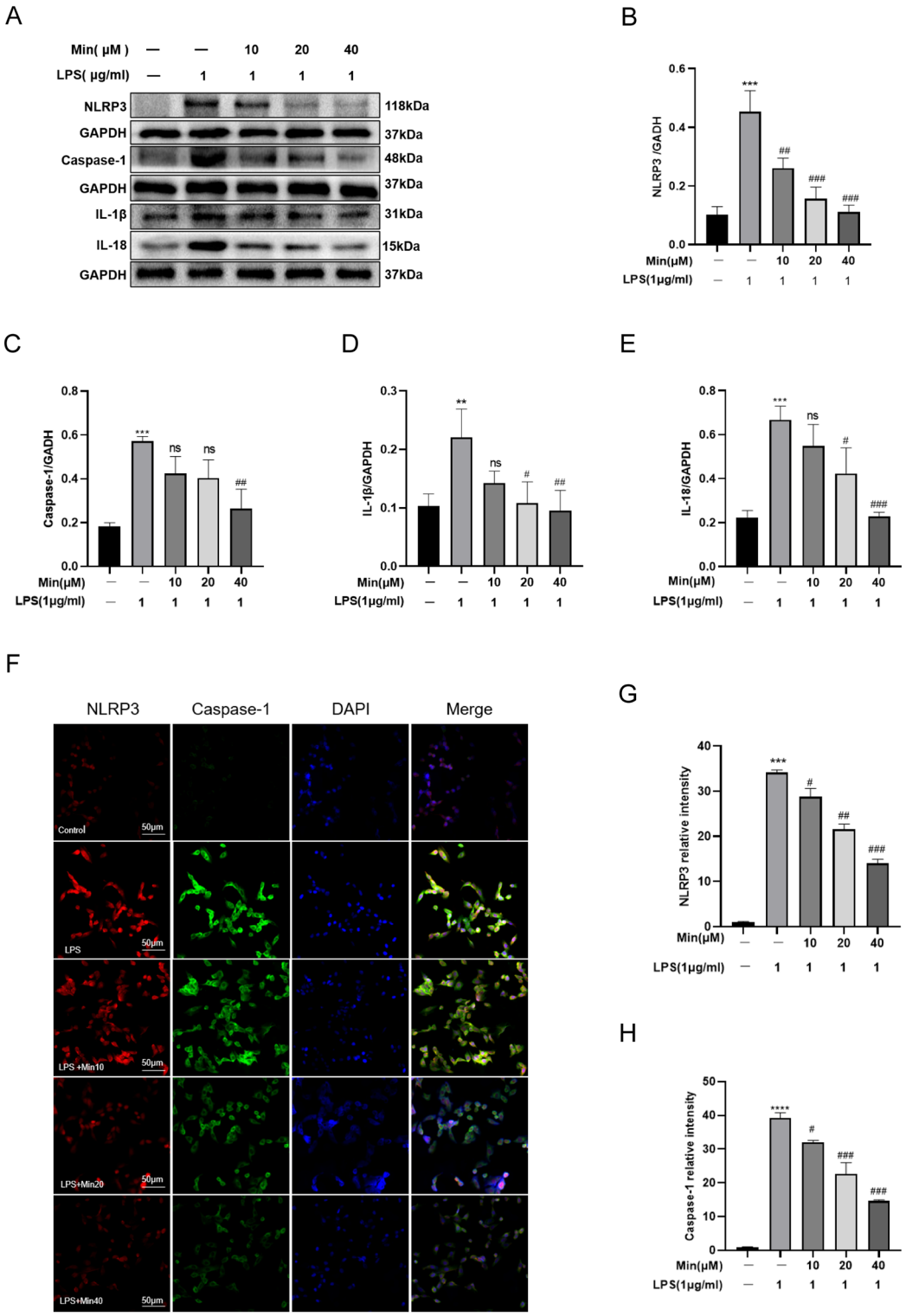

Fig. 6. Minocycline inhibits LPS-induced NLRP3/Caspase-1 signaling pathway activation in H9c2 cells. (**A**) Representative Western blot bands of NLRP3, Caspase-1, IL-1β, and IL-18, and (**B–E**) their statistical graphs. (**F**) Representative immunofluorescence images of NLRP3 and Caspase-1, and (**G,H**) their statistical graphs. Data were presented as mean ± SD; n = 3; ns: statistically non-significant, $^{*}P<0.05$, $^{**}P<0.01$, $^{***}P<0.001$ vs. control group; $^{\#}P<0.05$, $^{\#\#}P<0.01$, $^{\#\#\#}P<0.001$ vs. LPS group.

mitigate LPS-induced heart tissue injury and improve the viability of H9c2 cells. These results suggest that Min ameliorates LPS-induced SIC, potentially through inhibition of the NLRP3/Caspase-1 pathway.

Limitations

The study has several limitations. First, when examining markers of heart damage, we only examined LDH, not cTn together. While LDH is a commonly used marker of cell damage, it does not directly assess heart damage as cTn does. Therefore, we should consider measuring cTn in future studies to get a more complete picture of heart damage. Second, although HE staining, Western blotting, TUNEL and other methods were used to assess the effect of Min on cardiac tissue, hemodynamic measures such as ejection fraction and cardiac output would more intuitively assess the impact of our intervention on function. Therefore, we will incorporate these assessments in future studies to fully elucidate the impact of our findings on cardiac function. Third, our study focused solely on Min's effect on NLRP3/Caspase-1 expression, without manipulating or activating NLRP3 and Caspase-1 expression in vivo and in vitro, thus providing compelling evidence for the specificity and potency of Min's action through this signaling axis. In addition, our examination only delved into Min's function in H9c2 cells, neglecting its impact on other cardiac cell types like endothelial cells. Therefore, further extensive studies and experiments are necessary to intricately dissect the pathogenesis of lipopolysaccharide-induced SIC.

Conclusion

The study found that minocycline could relieve LPS-induced systemic inflammatory response syndrome (SIC) by blocking the NLRP3/Caspase-1 pathway. This indicates that minocycline may be a beneficial new treatment option for SIC.

Data availability

If anyone would like to request data from this study, please contact the corresponding author (Fenfang Zhan).

Received: 5 July 2024; Accepted: 4 September 2024
Published online: 11 September 2024

References

1. Singer, M. *et al.* The Third International Consensus definitions for sepsis and septic shock (Sepsis-3). *Jama* **315**(8), 801–810 (2016).
2. Merx, M. W. & Weber, C. Sepsis and the heart. *Circulation* **116**(7), 793–802 (2007).
3. Angus, D. C. *et al.* Epidemiology of severe sepsis in the United States: Analysis of incidence, outcome, and associated costs of care. *Crit. Care Med.* **29**(7), 1303–1310 (2001).
4. Romero-Bermejo, F. J., Ruiz-Bailen, M., Gil-Cebrian, J. & Huertos-Ranchal, M. J. Sepsis-induced cardiomyopathy. *Curr. Cardiol. Rev.* **7**(3), 163–183 (2011).
5. Flynn, A., Chokkalingam Mani, B. & Mather, P. J. Sepsis-induced cardiomyopathy: A review of pathophysiologic mechanisms. *Heart Fail. Rev.* **15**(6), 605–611 (2010).
6. Hollenberg, S. M. & Singer, M. Pathophysiology of sepsis-induced cardiomyopathy. *Nat. Rev. Cardiol.* **18**(6), 424–434 (2021).
7. Suzuki, T. *et al.* Sepsis-induced cardiac dysfunction and β-adrenergic blockade therapy for sepsis. *J. Intensive Care* **5**, 22 (2017).
8. Mantzarlis, K., Tsolaki, V. & Zakynthinos, E. Role of oxidative stress and mitochondrial dysfunction in sepsis and potential therapies. *Oxidat. Med. Cell. Longev.* **2017**, 5985209 (2017).
9. Kokkinaki, D. *et al.* Chemically synthesized Secoisolariciresinol diglucoside (LGM2605) improves mitochondrial function in cardiac myocytes and alleviates septic cardiomyopathy. *J. Mol. Cell. Cardiol.* **127**, 232–245 (2019).
10. Peng, Z., Zhang, W., Qiao, J. & He, B. Melatonin attenuates airway inflammation via SIRT1 dependent inhibition of NLRP3 inflammasome and IL-1β in rats with COPD. *Int. Immunopharmacol.* **62**, 23–28 (2018).
11. Kelley, N., Jeltema, D., Duan, Y. & He, Y. The NLRP3 inflammasome: An overview of mechanisms of activation and regulation. *Int. J. Mol. Sci.* **20**(13), 12 (2019).
12. Sharma, B. R. & Kanneganti, T. D. NLRP3 inflammasome in cancer and metabolic diseases. *Nat. Immunol.* **22**(5), 550–559 (2021).
13. Busch, K. *et al.* Inhibition of the NLRP3/IL-1β axis protects against sepsis-induced cardiomyopathy. *J. Cachexia Sarcopenia Muscle* **12**(6), 1653–1668 (2021).
14. Gunn, G. B. *et al.* Minocycline for symptom reduction during radiation therapy for head and neck cancer: A randomized clinical trial. *Supp. Care Cancer* **28**(1), 261–269 (2020).
15. Metz, L. M. *et al.* Trial of minocycline in a clinically isolated syndrome of multiple sclerosis. *N. Engl. J. Med.* **376**(22), 2122–2133 (2017).
16. Abdo Qaid, E. Y., Abdullah, Z., Zakaria, R. & Long, I. Minocycline mitigates tau pathology via modulating the TLR-4/NF-κβ signalling pathway in the hippocampus of neuroinflammation rat model. *Neurol. Res.* **2023**, 1–11 (2023).
17. Hosseini, M. *et al.* Minocycline mitigated enduring neurological consequences in the mice model of sepsis. *Behav. Brain Res.* **2024**, 114856 (2024).
18. Naderi, Y. *et al.* Cardioprotective effects of minocycline against doxorubicin-induced cardiotoxicity. *Biomed. Pharmacother.* **158**, 114055 (2022).
19. Qi, Z. *et al.* microRNA-130b-3p attenuates septic cardiomyopathy by regulating the AMPK/mTOR signaling pathways and directly targeting ACSL4 against ferroptosis. *Int. J. Biol. Sci.* **19**(13), 4223–4241 (2023).
20. Kang, W. *et al.* Neuregulin-1 protects cardiac function in septic rats through multiple targets based on endothelial cells. *Int. J. Mol. Med.* **44**(4), 1255–1266 (2019).
21. Naderi, Y. *et al.* Cardioprotective effects of minocycline against doxorubicin-induced cardiotoxicity. *Biomed. Pharmacother.* **158**, 114055 (2023).
22. Yi, Q. *et al.* Minocycline protects against myocardial ischemia/reperfusion injury in rats by upregulating MCPIP1 to inhibit NF-κB activation. *Acta Pharmacol. Sin.* **40**(8), 1019–1028 (2019).
23. Fu, Y., Zhang, H. J., Zhou, W., Lai, Z. Q. & Dong, Y. F. The protective effects of sophocarpine on sepsis-induced cardiomyopathy. *Eur. J. Pharmacol.* **950**, 175745 (2023).
24. Chen, Z. *et al.* TMEM43 protects against sepsis-induced cardiac injury via inhibiting ferroptosis in mice. *Cells* **11**(19), 133 (2022).
25. Zhang, M., Zhi, D., Liu, P., Wang, Y. & Duan, M. Protective effects of Dioscin against sepsis-induced cardiomyopathy via regulation of toll-like receptor 4/MyD88/p65 signal pathway. *Immun. Inflamm. Dis.* **12**(5), e1229 (2024).
26. Zhang, X. *et al.* FNDC5 alleviates oxidative stress and cardiomyocyte apoptosis in doxorubicin-induced cardiotoxicity via activating AKT. *Cell Death Differ.* **27**(2), 540–555 (2020).

27. Devasagayam, T. P., Boloor, K. K. & Ramasarma, T. Methods for estimating lipid peroxidation: An analysis of merits and demerits. *Indian J. Biochem. Biophys.* **40**(5), 300–308 (2003).
28. Song, C. *et al.* HSP70 alleviates sepsis-induced cardiomyopathy by attenuating mitochondrial dysfunction-initiated NLRP3 inflammasome-mediated pyroptosis in cardiomyocytes. *Burns Trauma* **10**, tkac043 (2022).
29. Joshi, S. *et al.* Anti-inflammatory activity of carvacrol protects the heart from lipopolysaccharide-induced cardiac dysfunction by inhibiting pyroptosis via NLRP3/Caspase1/Gasdermin D signaling axis. *Life Sci.* **324**, 121743 (2023).
30. Lin, X. *et al.* Quercetin ameliorates ferroptosis of rat cardiomyocytes via activation of the SIRT1/p53/SLC7A11 signaling pathway to alleviate sepsis-induced cardiomyopathy. *Int. J. Mol. Med.* **52**(6), 134 (2023).
31. Guo, S. & Guo, Q. Syphilis-associated septic cardiomyopathy: Case report and review of the literature. *BMC Infect. Dis.* **21**(1), 33 (2021).
32. Chen, X. S. *et al.* Losartan attenuates sepsis-induced cardiomyopathy by regulating macrophage polarization via TLR4-mediated NF-κB and MAPK signaling. *Pharmacol. Res.* **185**, 106473 (2022).
33. Hu, H. *et al.* Interleukin-35 pretreatment attenuates lipopolysaccharide-induced heart injury by inhibition of inflammation, apoptosis and fibrotic reactions. *Int. Immunopharmacol.* **86**, 106725 (2020).
34. Li, X. *et al.* Icariside II alleviates lipopolysaccharide-induced acute lung injury by inhibiting lung epithelial inflammatory and immune responses mediated by neutrophil extracellular traps. *Life Sci.* **3**, 122648 (2024).
35. Wei, A. *et al.* Syringaresinol attenuates sepsis-induced cardiac dysfunction by inhibiting inflammation and pyroptosis in mice. *Eur. J. Pharmacol.* **913**, 174644 (2021).
36. Zhou, Y. *et al.* Propofol mitigates sepsis-induced brain injury by inhibiting ferroptosis via activation of the Nrf2/HO-1axis. *Neurochem. Res.* **2024**, 15 (2024).
37. Zhu, X. X. *et al.* Cichoric acid ameliorates sepsis-induced acute kidney injury by inhibiting M1 macrophage polarization. *Eur. J. Pharmacol.* **976**, 176696 (2024).
38. Mercado-Gómez, M. *et al.* The lipopolysaccharide-TLR4 axis regulates hepatic glutaminase 1 expression promoting liver ammonia build-up as steatotic liver disease progresses to steatohepatitis. *Metab. Clin. Exp.* **13**, 155952 (2024).
39. Li, J., Teng, D., Jia, W., Gong, L., Dong, H., Wang, C. et al. PLD2 deletion ameliorates sepsis-induced cardiomyopathy by suppressing cardiomyocyte pyroptosis via the NLRP3/caspase 1/GSDMD pathway. *Inflamm. Res.* (2024).
40. Lu, J. S., Wang, J. H., Han, K. & Li, N. Nicorandil regulates ferroptosis and mitigates septic cardiomyopathy via TLR4/SLC7A11 signaling pathway. *Inflammation* **47**(3), 975–988 (2024).
41. Zhan, F. *et al.* Minocycline alleviates LPS-induced cognitive dysfunction in mice by inhibiting the NLRP3/caspase-1 pathway. *Aging* **16**, 34 (2024).
42. Cui, N. *et al.* Minocycline attenuates oxidative and inflammatory injury in a intestinal perforation induced septic lung injury model via down-regulating lncRNA MALAT1 expression. *Int. Immunopharmacol.* **100**, 108115 (2021).
43. Conway-Morris, A., Wilson, J. & Shankar-Hari, M. Immune activation in sepsis. *Crit. Care Clin.* **34**(1), 29–42 (2018).
44. Rivera, A., Siracusa, M. C., Yap, G. S. & Gause, W. C. Innate cell communication kick-starts pathogen-specific immunity. *Nat. Immunol.* **17**(4), 356–363 (2016).
45. Drosatos, K. *et al.* Pathophysiology of sepsis-related cardiac dysfunction: Driven by inflammation, energy mismanagement, or both?. *Curr. Heart Fail. Rep.* **12**(2), 130–140 (2015).
46. Chen, H. *et al.* Hydrogen alleviates mitochondrial dysfunction and organ damage via autophagy-mediated NLRP3 inflammasome inactivation in sepsis. *Int. J. Mol. Med.* **44**(4), 1309–1324 (2019).
47. Zhang, W. *et al.* Cardiac fibroblasts contribute to myocardial dysfunction in mice with sepsis: The role of NLRP3 inflammasome activation. *PloS one* **9**(9), e107639 (2014).
48. Yang, L., Zhang, H. & Chen, P. Sulfur dioxide attenuates sepsis-induced cardiac dysfunction via inhibition of NLRP3 inflammasome activation in rats. *Nitric Oxide Biol. Chem.* **81**, 11–20 (2018).

Acknowledgements

The authors would like to thank all the reviewers who participated in the review.

Author contributions

Hui-juan Li: Data curation, Writing-original draft preparation ; Xiao-zhong Li: Investigation, Data curation.; Guo-hai Xu: Funding acquisition, Conceptualization, Methodology; Fen-fang Zhan reviewing and editing, Software. All authors reviewed the manuscript.

Funding

This study was supported by the National Natural Science Foundation of China (81760208 and 81760261) and the Key Laboratory of Anesthesiology of Jiangxi Province (20164BCD40093).

Competing interests

The authors declare no competing interests.

Ethical approval

The animal study was performed in accordance with ARRIVE relevant guidelines and regulations, and was approved by the Institutional Animal Care and Use Committee at the Medical College of Nanchang University Approval. All methods were carried out in accordance with relevant guidelines and regulations.

Additional information

Supplementary Information The online version contains supplementary material available at https://doi.org/10.1038/s41598-024-72133-4.

Correspondence and requests for materials should be addressed to F.Z.